ELSEVIER

Chemical Geology 244 (2007) 175–185

CHEMICAL GEOLOGY
INCLUDING ISOTOPE GEOSCIENCE

www.elsevier.com/locate/chemgeo

A comparative Raman spectroscopic study of natural gas hydrates collected at different geological sites

Bertrand Chazallon [a,*], Cristian Focsa [a], Jean-Luc Charlou [b], Christophe Bourry [b], Jean-Pierre Donval [b]

[a] *Laboratoire de Physique des Lasers, Atomes et Molécules (PhLAM), Université Lille 1, UMR CNRS 8523, CERLA FR-CNRS 2416, 59655 Villeneuve d'Ascq, France*

[b] *Département Géosciences Marines, IFREMER, Centre de Brest, 29280 Plouzané, France*

Received 29 September 2006; received in revised form 8 June 2007; accepted 9 June 2007

Editor: J. Fein

Abstract

Intact natural gas hydrates recovered on the West African margin in the South Atlantic Ocean (ZaiAngo and Neris II projects) and from the Norwegian Sea (Hakon Mosby Mud Volcano) are investigated by micro-Raman spectroscopy at ambient pressure and low temperature. The gas hydrates collected at different geological sites contain a high methane concentration relative to other minor components that are slightly dispersed in the samples. They crystallize in a type I cubic lattice structure as also confirmed by our preliminary synchrotron diffraction results obtained on the ZaiAngo specimen. However, detailed analysis of selected microscopic areas reveals a variation in the gas distribution among the different specimens. Trace amounts of CO_2 and H_2S can be identified by their characteristic vibrational signatures in the 1000–3800 cm^{-1} spectral range. They are found to be co-clathrated with methane. Their presence produces a compositional effect on the relative cage occupancy of CH_4, as determined from the integrated band intensity ratio corresponding to the molecular stretching modes of methane in the hydrate. The comparative Raman analysis of synthetic hydrates of H_2S, CH_4 and CH_4-deuterohydrates allows the unambiguous assignment of weak band overtones of trapped methane and co-clathrated H_2S molecular vibrations.

Keywords: Natural clathrate hydrates; CH_4-hydrate; H_2S-hydrate; Micro-Raman spectroscopy

1. Introduction

Gas hydrates (clathrates) occur naturally on Earth, generally where suitable conditions of high pressure (p) and low temperature (T) prevail. The required p–T conditions for their formation are encountered in marine sediments mainly offshore along continental margins, and to a lesser extent in polar regions commonly associated with permafrost (Kvenvolden, 1998; Kvenvolden and Lorenson, 2001). They are non-stoichiometric crystalline ice-like compounds with a host lattice composed of hydrogen-bonded water molecules forming cages of different sizes that can accommodate gas molecules (guest). Natural gas hydrates can crystallize in different structure types depending on the nature and size of the guests involved. The unit cell of a cubic type I structure (sI) with space group $Pm\bar{3}n$ comprises 46 H_2O molecules and consists of two small cages (SC) (pentagonal dodecahedral) and six large cages (LC)

* Corresponding author. Laboratoire de Physique des Lasers, Atomes et Molécules, Université des Sciences et Technologies de Lille, 59655 Villeneuve d'Ascq Cedex, France. Tel.: +33 320336468; fax: +33 320336463.

E-mail address: chazallon@phlam.univ-lille1.fr (B. Chazallon).

0009-2541/$ - see front matter © 2007 Elsevier B.V. All rights reserved.
doi:10.1016/j.chemgeo.2007.06.012

(tetracaidecahedral) (Stackelberg, 1949). The occluded guest molecules stabilize the host framework and are statistically distributed among the different cages with a maximum of one molecule per cage (van der Waals and Platteuw, 1959). Exception to this rule and the presence of doubly occupied cages has been evidenced experimentally in type II N_2-, O_2- and air-hydrates (Kuhs et al., 1997; Chazallon and Kuhs, 2002). This topologically related cubic structure II (with space group $Fd\bar{3}m$) consists of 136 H_2O water molecules that form 16 small dodecahedral cages and 8 large hexacaidecahedral cages. Extreme conditions favourable to natural air-hydrates formation are encountered in polar ice cores where air-bubbles trapped in the upper part of the ice sheet slowly transform due to the increasing pressure at high depth (Miller, 1969). Consequently, these hydrates provide a potentially continuous record of past atmospheric composition (Miller, 1969; Shoji and Langway, 1982).

Considerable amounts of natural gases such as methane (a type I hydrate former) are expected to be trapped in the form of clathrates in deep water regions. These compounds represent a considerable energy reserve that corresponds to more than 50% of the world's recoverable reserve of organic carbon (Lee and Holder, 2001). They are therefore very attractive for the gas industry which starts to provide possible future approaches to their exploitation. In contrast to this attractive approach, their role has been repeatedly quoted in geological hazards (McIver, 1982) or global climate change (Kvenvolden, 1993). Indeed, different speculative scenarios still sustain discussion to explain the possible role of methane hydrate in past and future global climate change (Nisbet, 1990; Paull et al., 1991) due to the potentially enormous "greenhouse" feedback effect of methane (Kvenvolden, 1999).

The physical properties of natural gas hydrates are important to develop technologies for their exploitation or to establish their formation/dissociation rates and stability fields. Even if laboratory experiments on synthesized gas hydrates are necessary for this purpose, they cannot offer a complete picture of the complex natural processes peculiar to hydrates formation and composition in deep-sea environment. Indeed, the conditions of crystallization and reactants in nature are very different from idealized laboratory experiments and may lead to the formation of a different product. Although new gas hydrate sites are discovered regularly, cores containing intact gas hydrates could only be recovered from 27 oceanic sites (Kvenvolden, 1999), partly due to their instability at ambient temperature and pressure and to the technological difficulties to recover natural solid samples at high depth. In most of the laboratory work on the recovered specimens, the presence of gas hydrates was inferred indirectly from the quantity and nature of the gaseous decomposition products (Kvenvolden et al., 1984; Brooks et al., 1988; Sassen and McDonald, 1994). Only a limited number of analyses have been performed using more direct methods of characterization. They concern intact natural hydrates recovered from sediment cores originating from Gulf of Mexico (Davidson et al., 1986; Yousuf et al., 2004), Blake Ridge (Uchida et al., 1999), Mallik (Tulk et al., 2000), Northeast Pacific continental margin off Oregon (Gutt et al., 1999), Cascadia margin (Yousuf et al., 2004) and more recently Okhotsk Sea (Takeya et al., 2006). Moreover, recent development has been conducted in order to probe in-situ ocean clathrate hydrates via Raman spectroscopy (Hester et al., 2006). All these studies revealed the presence of different structures in these heterogeneous environments and stressed the importance to study the intact solid (un-decomposed and undisturbed in the subsurface). Our previous report was focused on the physical and chemical characterization of intact gas hydrates collected in the Congo–Angola basin (Charlou et al., 2004). The present work extends this study to gas hydrates collected in two new areas: the Nigerian and Norwegian margin. A detailed Raman analysis of spectral features corresponding to the internal vibrational motion of the gas molecules is presented. Laboratory specimens of hydrogen sulphide (H_2S)-hydrate and methane (CH_4)-hydrate/deuterohydrate are analysed to allow a better identification of the occluded gases and to circumvent ambiguities that may arise in the assignment of weak overtone bands occurring in natural hydrates.

2. Experimental methods

2.1. Sample storage and preparation

Gas hydrates from the Congo–Angola basin (ZAI–ROV cruise, Dec. 2000) (Savoye et al., 2000) were collected from a deep giant pockmark (~1 km in diameter) on the ocean floor at 3160 m water depth in a 12 m long sediment core. Hydrates up to 10 cm in diameter were extracted from the core barrel. Smaller specimens were found disseminated over a 50 cm long zone in the sediment (Charlou et al., 2004). The recovered pieces (massive hydrates) were first stored at 190 K on board before being shipped to France for further laboratory analysis. The second specimens examined were recovered from the passive Nigerian margin (NERIS II cruise, Dec. 2003) 500 km north from the previous studied area at ~1200 m water depth in a 1–3 m sediment core. The sample presents some amber colored part on the surface, generally associated with the presence of oil, bacteria and

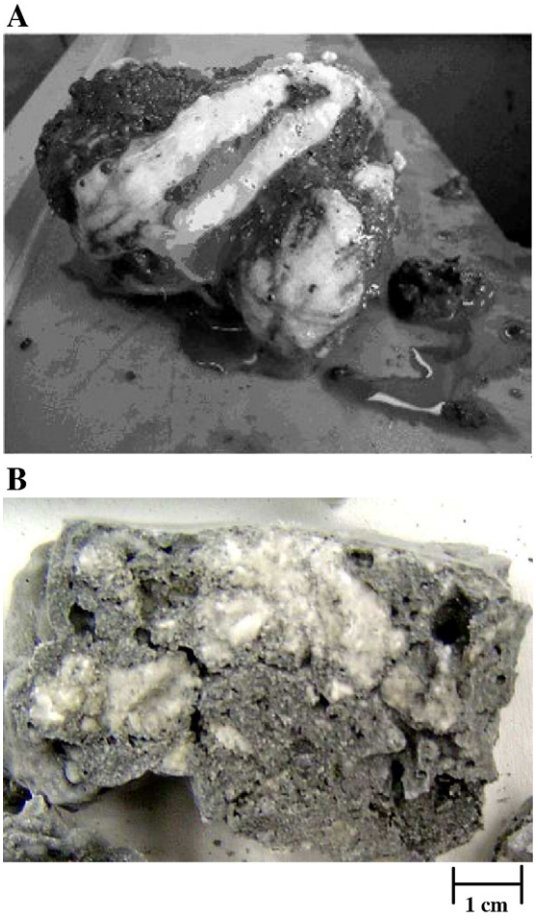

Fig. 1. Recovered gas hydrate samples from the Nigerian margin (A) and Norvegian site (B). The white and greyish-white vein fillings correspond to ice and hydrate mixtures embedded in the solid mud sediment.

minerals and is embedded in greyish sediments. Macroscopically, they appear as white vein-like forms surrounded by mud (Fig. 1A). The third set of samples originated from the Norwegian–Svalbard continental slope (with VICTOR 6000 ROV, 2003) on the Hakon Mosby Mud Volcano (HMMV) and were extracted at ~1260 m water depth in a ~3 m long sediment core before being stored at 190 K on board. Truncated portions of the solid reveal distinct white and greyish-white vein-filling zones (2–3 cm long) that correspond to the presence of hydrate and ice. This latter proves to be abundant in this sample and may have been induced by hydrate dissociation or gas expansion during recovery (Fig. 1B). All these samples are now preserved from decomposition in liquid nitrogen containers.

CH_4- and H_2S-hydrates and CH_4-deuterohydrate are produced synthetically in a high pressure stainless steel vessel of low volume capacity (~4 cm^3). Ice (H_2O or D_2O (99.9% deuterated, Aldrich)) is ground with a mortar and a pestle at low temperature before being inserted into the high pressure cell. A glove box filled with a dry nitrogen atmosphere is used for preparation of the deuterohydrate in order to limit the H/D exchange. The gas pressure (methane, 99.9%, Air Liquide) is subsequently raised up to 30 bar to initiate CH_4-hydrates formation. In this regime the hydrate remains in its stability zone. The vessel is then stored for 11 days in our cold room at −2 °C. The sample is recovered at low temperature and atmospheric pressure, and stored immediately in the vapour of liquid nitrogen before being analysed by Raman. H_2S-hydrate is synthesized similarly using a gas pressure (H_2S, 99.5% Air Liquide) of 15 bar. 8 days are allowed for hydrate formation at −2 °C in the cold room.

2.2. Characterization tools

The natural samples are analyzed by micro-Raman spectroscopy using two different instruments: an XY (DILOR) in Lyon and a LABRAM (Jobin–Yvon) in Lille. The synthetic samples are analyzed using a T64000 (Jobin Yvon) in Lille. About sixty Raman spectra were recorded for each sample. The gas hydrates are handled and quickly transferred in dry liquid nitrogen vapour before being loaded into a pre-cooled LINKAM TMS 600 stage. The working temperature is set between 90 and 130 K to preserve the samples from decomposition. The analyzed area corresponds to a circular beam spot size of 2 to 5 μm in diameter when using the ULWD × 50 Olympus objectives. Typical spectral resolutions of 7 cm^{-1} (LABRAM) and 1 cm^{-1} (XY and T64000) are chosen by adjusting the entrance slit width. The laser power at the sample is ~5 mW, thus avoiding sample damage under the laser irradiation. Further details on the loading procedure can be found elsewhere (Chazallon et al., 1998). The peak positions are calibrated using emission lines of a neon lamp. The spectra are then baseline corrected and analyzed with a least-square fitting protocol (PeakFit4) using Voigt area profiles. This procedure allows a precise determination of the integrated band intensities for spectra collected with a high signal to noise ratio.

3. Results and discussion

3.1. Cage occupancies and structure

3.1.1. Spectral features of CH_4

A detailed physical and chemical characterization (using various techniques) of the gas hydrate and associated methane plumes from the *Congo–Angola basin*

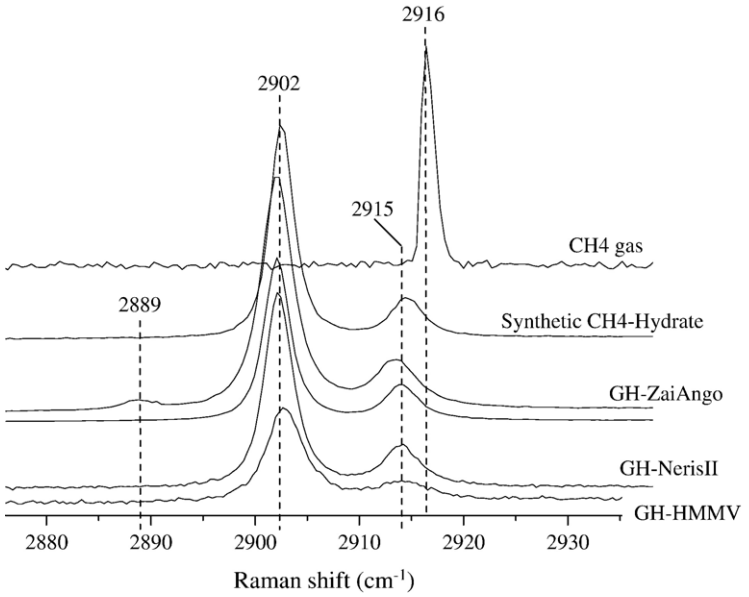

Fig. 2. Comparison between Raman spectra of natural hydrates collected at different sites and synthetic CH_4-hydrate. The spectral region corresponds to the C–H stretching of methane. The characteristic twin bands at ~2902 and ~2915 cm^{-1} are attributed to CH_4 trapped in the large and small cage of the type I structure. C–H stretching of methane gas (atmospheric pressure) with a unique band at ~2916 cm^{-1} is plotted for comparison. Note the occurrence of a component at ~2889 cm^{-1} attributed to C–H stretching of CH, CH_2, CH_3 group of aliphatic groups.

zone has been reported previously (Charlou et al., 2004). Sediment-free hydrates extracted from the inner part of this massive sample have been shown to contain up to ~99.1% methane. Fig. 2 shows typical Raman spectra of the different natural hydrates recorded at atmospheric pressure and 113 K in the 2875–2935 cm^{-1} spectral range. They are compared to the Raman spectra of the synthetic CH_4-hydrate and free methane gas (Fig. 2). Two bands of integrated intensities I_L and I_S can be observed respectively at ~2902 cm^{-1} and ~2915 cm^{-1}, for each gas hydrate. Their widths at half peak height (WHH) are ~3 cm^{-1} and ~4 cm^{-1} respectively. They correspond to the C–H stretching (ν_1 mode) of methane trapped in the type I hydrate structure. In comparison, only a single band corresponding to ν_1 is observed for methane in free gas phase at atmospheric pressure: ~2916 cm^{-1} with a WHH of ~1.5 cm^{-1} (Fig. 2).

The splitting of the ν_1 band in the hydrates can be attributed to a perturbation of the local electrostatic fields produced by the water molecules forming cages of different types (Tulk et al., 2000). The peak at ~2902 cm^{-1} can be assigned to the C–H stretching of CH_4 within the LC whereas the peak at ~2915 cm^{-1} to the C–H stretching of methane within the SC, in agreement with previous Raman experiments on synthetic CH_4-hydrates (Sum et al., 1997). The "loose-cage–tight-cage" model developed by Pimentel and Charles (1963) and revisited recently by Subramanian and Sloan (2002) corroborates these assignments and qualitatively predicts a more negative frequency shift (relative to the gas phase) for molecules in a "loose cage" environment such as methane in a LC. In contrast, CH_4 in the SC is trapped in a "tighter cage" environment, and the band at ~2915 cm^{-1} is found closer to the C–H stretch of the free methane gas. Actually, it is stipulated that the frequency shift relative to the gas phase depends on the location of the guest molecule relative to the water cage wall through the first and second derivatives of the guest–host interaction potential. For certain distances of methane from the wall both derivatives are negative and the stretching frequencies are thus found at lower values when compared to the free gas phase. This applies to the methane hydrogen atoms located at distances satisfying this condition. The tighter SC environment experienced by trapped CH_4 when compared to the situation in the LC leads to a less negative C–H frequency shift due to changes in the magnitudes of the potential derivatives.

3.1.2. Methane hydrate occupancy ratios

The integrated intensity ratio I_S/I_L is useful to discriminate between the different clathrate structure types and is representative of the cage occupancy ratio. In a type I structure there are three times as many large cages as small cages and the theoretical cage occupancy ratio θ_{SC}/θ_{LC} is thus obtained by $3I_S/I_L$, where θ_{SC} and θ_{LC} are the fractional occupancies of the small cage and

Table 1
Relative cage occupancy of methane trapped in the hydrate structure I as determined from Raman band corresponding to C–H stretching

Hydrate	θ_{SC}/θ_{LC}
ZaiAngo	0.86±0.03
Neris II	0.81±0.02
HMMV	0.8±0.1
CH_4-hydrate	0.78±0.02
H_2S-hydrate	0.95±0.1

large cage, respectively (Sum et al., 1997). We assume here that the relative Raman cross-sections of CH_4 and polarizabilities in both types of cage are similar. These assumptions are however not obvious and the ν_1 splitting of ~12 cm^{-1} may in turn reflect a perturbation of the C–H bond length, i.e. of the scattering cross-section, as discussed by Tulk et al. (2000). Using a cross-calibration of Raman and NMR, Wilson et al. (2002) show in turn that the cage occupancy ratio deduced from Raman experiments is quantitative for pure sI methane hydrate. But this situation apparently differs for binary CH_4/CO_2 systems, where the occupancy ratio is only found qualitative and varied by ~11% from the NMR results. This may reflect the influence of CO_2 in the neighbouring cages that affects the polarizability derivatives (i.e. also the relative intensities in the Raman spectra) of the CH_4 molecule. However, this result was obtained for a system with a much higher CO_2 concentration than those reported in our study. Therefore, we believe that the small amounts of minor components could only weakly affect the Raman scattering cross-section and that θ_{SC}/θ_{LC} is here quantitative.

For the ZaiAngo hydrate, we refine our previous data treatment and investigate additional data to obtain an experimental θ_{SC}/θ_{LC} ratio of 0.86±0.03 (Table 1). This value is close to the one (0.79) obtained by Uchida et al. (1999) on a natural gas hydrate recovered from the ODP Leg 164 at Blake Ridge. A somewhat lower ratio is obtained for the NERIS II — hydrate with $\theta_{SC}/\theta_{LC}=0.81\pm0.02$. Note that the methane signal can be detected already at the sample surface, thus indicating a rather good preservation of this specimen. θ_{SC}/θ_{LC} for the HMMV hydrate is less precise with a standard deviation relatively higher than the others (Table 1). Hydrates previously recovered from this area have been inferred to contain up to 99.9% methane (Milkov et al., 2004). Unfortunately, the storage conditions were different for this sample as it was maintained at ~190 K during several months, before being analyzed in Lille. Therefore, partial decomposition and the release of methane may have occurred during this period. It thus explains the difficulties to locate hydrate-rich zones and the abundant presence of crystalline ice. Moreover, no other gas components can be detected using our Raman technique (detection limit ≲1%) and we have therefore considered that the methane concentration is the one determined by Milkov et al. (2004).

For the synthetic CH_4-hydrate a ratio of $\theta_{SC}/\theta_{LC}=0.78\pm0.02$ is obtained. This result indicates that the SCs are relatively less occupied by methane molecules than the LCs. This view is consistent with a deviation from an ideal Langmuir behaviour for the SC as reported recently on artificial CH_4-hydrate (Klapproth et al., 2003). Further, our result is close to that obtained by Uchida et al. (1999) on synthetic hydrates using similar conditions of formation (29.5 bar and 273.6 K) with $\theta_{SC}/\theta_{LC}=0.77\pm0.02$. Note that no significant variation in the ratio is to be expected for higher hydrate formation pressure (up to ~1 kbar) (Klapproth, 2002). One infers that the slightly higher ratio obtained for the ZaiAngo-hydrate may reflect the presence of other gas components occupying the LC, thus reducing the population of methane in the LC. The ZaiAngo hydrate was previously shown to contain ~1% CO_2 (as also detected by Raman) and other minor gas components such as C_2H_6 (0.043%) and H_2S (0.02%) as obtained from gas chromatography analysis of a bulk portion of the specimen (Charlou et al., 2004). As CO_2 preferentially partitions into the LC (Kuhs et al., 1998; Udachin et al., 2001), the relative occupancy ratio of methane may be slightly affected in this hydrate. The intensity of the CO_2 bands is seen to vary slightly from point to point. This means that CO_2 is heterogeneously dispersed in the specimen. The standard deviations associated with the estimates of θ_{SC}/θ_{LC} (Table 1) are related to this variation. In contrast, the Neris II hydrate is shown to consist of almost pure methane (Charlou, private communication) with the presence of trace elements such as H_2S (see below), while very weak signals of CO_2 can be detected. Its composition thus merely reflects that of a pure methane hydrate. Further work using mixed gas components is needed to confirm the trend observed.

Moreover, on a localized part of the sample, one extra component at ~2889 cm^{-1} is also observed on the ZaiAngo specimen (Fig. 2). This band may be attributed to C–H stretching of CH, CH_2 or CH_3 groups of aliphatic groups (Ferraro and Nakamoto, 1994) and may characterize the presence of high hydrocarbons or oil and olefins. It is noted that no CO_2 can be detected in this zone whereas a slight decrease of θ_{SC}/θ_{LC} of CH_4 is observed (~0.79), thus corroborating our interpretation.

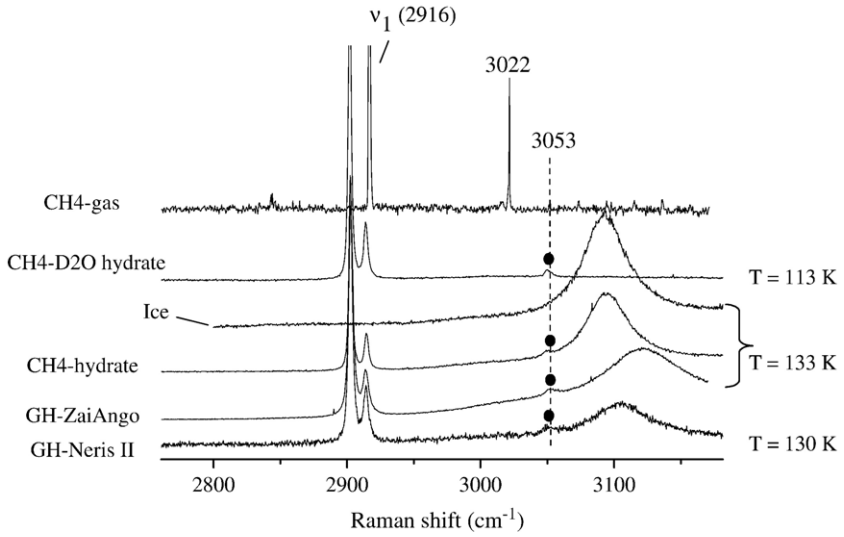

Fig. 3. Comparative spectra of the O–H spectral region of water at ~3100 cm^{-1}. The weak additional component at ~3053 cm^{-1} characterizes the presence of hydrates. It is assigned to an overtone of methane (see text). Its presence is confirmed on the spectra of the CH_4-deuterohydrate where the contribution of water molecules (O–D stretching) are absent from the spectral region. Variations in the O–H band position is due to differences in temperature and/or reflect the structural differences between ice and hydrate which are both present in the variable amounts under the laser spot. The spectra of methane in the free gas phase is shown for comparison (see Results and discussion).

The average value of θ_{SC}/θ_{LC} given in Table 1 for the ZaiAngo specimen does not include this particular case. Moreover, our preliminary structural investigation obtained by synchrotron X-ray diffraction at ambient pressure and ~90 K reveals the presence of only two independent phases: ice Ih (~73 wt.%) and type I (~27 wt.%) with a lattice constant of $a = 11.869522(23)$ Å for type I. Further work is in progress on the thermal evolution of the lattice parameters and structural stability of the different hydrates. This will be addressed in a separate contribution.

3.2. O–H stretching spectral region and weak bands attribution

The O–H spectral region of water at ~3100 cm^{-1} is displayed in Fig. 3. It shows an additional small component at ~3053 cm^{-1} on the low frequency side of the broad band corresponding to the O–H symmetric stretching in the hydrate. This band does not appear on the spectrum of pure ice (Fig. 3). Our previous assignment was based on the probable presence of some aromatic groups in small quantities in the environment of the gas hydrates (e.g. benzene and derivatives, olefins) (Charlou et al., 2004). This was in line with previous works on CH_4-rich inclusions that attributed the corresponding spectral feature to high hydrocarbons (Wopenka et al., 1990; Kisch and van den Kerkhof, 1991). We propose here another interpretation and provide further rationales for our assignment, which are based on the comparison with our synthetic pure CH_4-hydrate/deuterohydrate results. In Fig. 3, the O–H spectral region of the artificial CH_4-hydrate displays a weak band at ~3053 cm^{-1}, in agreement with previous Raman spectra of CH_4-hydrate obtained independently (Schicks et al., 2005). Given the high purity of our sample, this band originates from a molecular vibration of methane trapped in the hydrate structure. This is further confirmed on the CH_4-deuterohydrate spectra (Fig. 3) where the contribution of the water (O–D) stretching is shifted in the ~2300 cm^{-1} spectral range (not shown on the figure), while the contribution at ~3053 cm^{-1} still remains. A precise assignment to a methane internal molecular motion is however not straightforward. In comparison, a weak band is observed for methane in the gas phase (Fig. 3, Table 2) at ~3022 cm^{-1} that corresponds to the triply degenerate anti-symmetric C–H stretching. Moreover, at higher pressure (above 2 bar) a weak overtone starts to grow at ~3070 cm^{-1} (Brunsgaard Hansen et al., 2001; Hester et al., 2006). On the basis of group theory, this is attributed to an overtone of the doubly degenerate vibration ν_2 (~1540 cm^{-1}, bending) of methane (Table 2). CH_4 belongs to the point group T_d (T_d represents the set of symmetry operations of CH_4 and satisfying the properties of a group in mathematical sense (Colthup

Table 2
Wavenumbers and assignments of the Raman bands of CH_4 and H_2S in the gas phase and in the hydrate phase

Gas component	Assignment proposed [a]	Symmetry	Hydrate sI (this work)
CH_4/ν (cm^{-1}) [b]		T_d point group	CH_4/ν (cm^{-1})
1306 (I)	$\underline{\nu_4}$ bending	F_2	–
1540 (R)	$\underline{\nu_2}$ antisym. bend	E	–
2605	$2\nu_4$ overtone	A_1+E+F_2	2570.2
2917 (R)	$\underline{\nu_1}$ sym. C–H	A_1	2902.4 (LC) 2914.5 (SC)
3020 (I/R)	$\underline{\nu_3}$ antisym. C–H stretching	F_2	–
3070 (R)	$2\nu_2$ overtone	A_1+E	3052.7
H_2S/ν (cm^{-1}) [b]		C_{2v} point group	H_2S/ν (cm^{-1})
1183	$\underline{\nu_2}$ bending	A_1	–
2611	$\underline{\nu_1}$ sym. H–S stretching	A_1	2593.4 (LC) 2605.1 (SC)
(2627)	$\underline{\nu_3}$ antisym. stretching	B_2	–

[a] Gas phase, fundamentals internal modes are underlined.
[b] Theoretical in parenthesis (Nakamoto, 1978), observed by Raman = R, by Infrared = I.

et al., 1990)). According to T_d, this mode is active in Raman as deduced from the relation:

$$\chi_E^2(R) = \frac{1}{2}(\chi_E(R)\chi_E(R) + \chi_E(R^2)),$$

where $\chi_E^2(R)$ is the character corresponding to the symmetry operation R (in T_d) performed two times. It results that $E^2 = A_1 + E$. Since both A_1 and E fundamental vibrations are allowed in Raman, the first overtone of E type normal coordinates is also allowed and should be observed at $2\nu_2$ (~3070 cm^{-1}) (Brunsgaard Hansen et al., 2001). The perturbed local molecular environment due to water molecules in the hydrate may result in a shift of the frequency at ~3053 cm^{-1}. It should be noted that the fundamental ν_2 is very weak and is not observed by us. The fact that $2\nu_2$ is easily observable can be explained by a Fermi resonance effect due to a slight interaction of $2\nu_2$ with the strongest Raman line ν_1 (Herzberg, 1991). This effect results from the small frequency difference between $2\nu_2$ (overtone) and ν_1 (fundamental) that leads to an enhanced intensity for the bands corresponding to these modes. Other additional effects may contribute to the intensification of this overtone (see below). Therefore, the assignment of the ~3053 cm^{-1} band to $2\nu_2$ mode appears to us reliable. In contrast, it should be noted that the trend predicted by the loose-cage–tight-cage model (Subramanian and Sloan, 2002) for low frequency bending vibrations (and thus their overtones) is opposite. Actually, these modes are predicted to shift positively relative to the gas phase. On the basis of this model, one would thus expect a band corresponding to $2\nu_2$ at frequencies higher than 3070 cm^{-1}, a situation that we do not observe. However, it is known that the model, while generally applicable, cannot always explain trends in bending frequencies of the guests (e.g. partial agreement is given in the case of CO_2-hydrate and SO_2-hydrate) (Subramanian and Sloan, 2002). Furthermore, the model predicts that the band corresponding to ν_3 stretching would be shifted at frequencies lower than 3022 cm^{-1}, however, no band is observed below this value. A comparison with the situation in pure methane gas at high pressure may provide a valuable explanation. In the gas phase, the intensity ratio between the two bands corresponding to the anti-symmetric ν_3 mode and $2\nu_2$ bending overtone ($I(\nu_3)/I(2\nu_2)$) is shown to decrease substantially as pressure of methane increases (Brunsgaard Hansen et al., 2002). Moreover, it is reported that the intensity of the band corresponding to ν_3 mode becomes very weak between 300 and 400 bar and that $I(\nu_3)/I(2\nu_2)$ is independent of the presence of other natural gas components. Given that the methane density in the recovered hydrate is comparable to that occurring in the gas phase at high pressure, one may expect similarities in the evolution of the $I(\nu_3)$ band. Thus, it is likely that the Raman band intensity $I(\nu_3)$ becomes also very weak in the hydrate and fails to be detected with the present experimental set-up. Although probable, the presence of liquid hydrocarbons in the vicinity of these natural gas hydrates is finally not necessary to explain the spectral feature observed at ~3053 cm^{-1}.

3.3. Other gas components and weak bands

3.3.1. CO_2-hydrate

The Raman signature of CO_2-hydrate can be identified in the ZaiAngo specimen with two bands at ~1377 and ~1274 cm^{-1} (Charlou et al., 2004). These bands were attributed to the ν_1 (symmetric stretching O–C–O) and $2\nu_2$ (bending overtone) modes of the CO_2 molecules trapped in a type I structure, in agreement with Sum et al., 1997. They are shifted relative to the free CO_2 gas phase frequencies expected at 1388 and 1285 cm^{-1} (see inset of Fig. 4). For the gas hydrate of the Nigerian margin, traces of CO_2 can only be detected on some localized part of the sample thus corroborating a higher CH_4 purity for this hydrate.

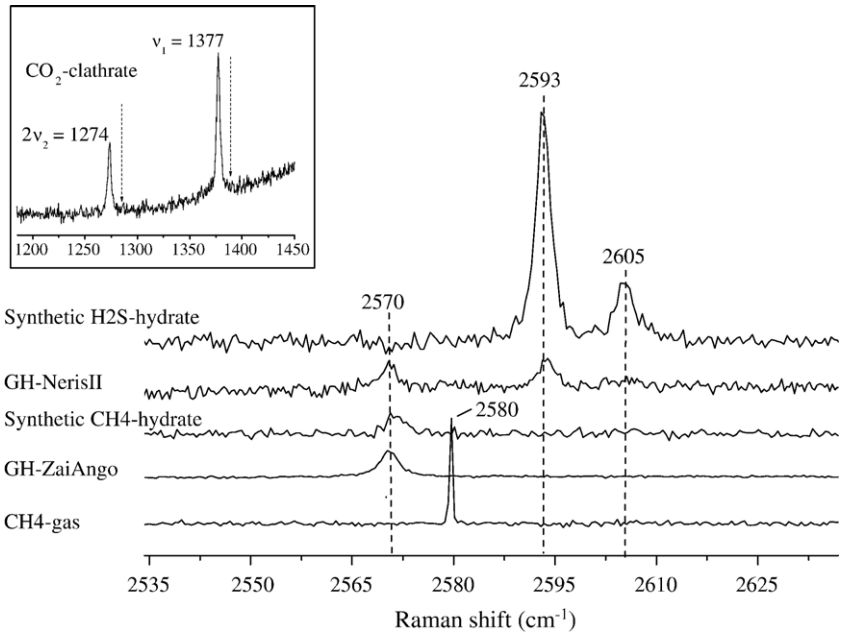

Fig. 4. Comparative Raman spectra corresponding to H–S spectral region. A unique component is observed for the gas hydrate from ZaiAngo and the synthetic CH_4-hydrate at ~2570 cm^{-1}, whereas an additional component at ~2593 cm^{-1} appears in the Neris II hydrate. This latter matches well that observed in the synthetic H_2S-hydrate (see text for the assignment). The inset shows the characteristic spectral lines of CO_2-clathrate (ν_1 and $2\nu_2$ stretching and overtone of the bending, respectively) observed in the ZaiAngo-hydrate. The vertical dotted lines represent the approximate positions of the corresponding bands expected for CO_2 in the gas phase.

3.3.2. H_2S-hydrate

A weak band is observed at ~2570 cm^{-1} (Fig. 4, Table 2) on the spectrum of the gas hydrate from Congo–Angola basin. This band is close to the spectral region of the molecular vibration (H–S stretching) of H_2S or HS^- molecules. These species are produced by the oxidation of methane in deep sea environments. Dissolved HS^- ions in water are known to have a contribution at ~2573 cm^{-1} and molecular H_2S at 2590 cm^{-1} (Rosasco and Roedder, 1979). An assignment to the H_2S-clathrate in our case is however not straightforward and should be considered with caution. The important shift (~40 cm^{-1}) relative to the free gas phase of H_2S (2611 cm^{-1} (Schrötter and Klöckner, 1979)) would suggest a rather strong interaction of H_2S with the cage wall, possibly arising from the formation to some extent of hydrogen bonding. IR-spectra of H_2S-clathrate hydrate at 10 K (Richardson et al., 1985) display a complex band system around 2550 cm^{-1} and 2610 cm^{-1}, assigned, respectively, to H–S stretching in the LC and in the SC. The sharp band system may indicate that H_2S assumes two or more different sites or orientations in both the SC and the LC at 10 K. It also differs significantly from the band obtained in the low temperature crystalline H_2S phases (Richardson et al., 1985). With a C_{2V} point group symmetry, all normal vibrational modes of the H_2S molecule are active in both IR and Raman. However, the Raman analysis of our synthetic H_2S-hydrate yields two bands at ~2593 cm^{-1} and ~2605 cm^{-1} with a WHH of ~2.5 cm^{-1} and ~3 cm^{-1}, respectively (Fig. 4, Table 2). Assuming a type I structure in the conditions of their formation (Davidson, 1973), they can be assigned to the H–S stretching in the LC and in the SC, respectively. It is noted that H_2S has apparently a higher tendency to be incorporated in the SC of the type I than CH_4 or CO_2 as can be deduced from the higher relative cage occupancy ratio (Table 1). The band assignment proposed is in agreement with the one reported previously by Raman on synthetic fluid inclusions of water and H_2S (Dubessy et al., 1992). The discrepancies between IR and Raman techniques remain however unexplained. It should be noted that a different protocol was used to form H_2S-hydrate in the IR experiment. The crystalline compound results from the vapour co-deposition at low temperature of an appropriate water/gas ratio and subsequent thermal treatment between 130 K and 10 K. Further work using Raman and samples produced by co-deposition will help to elucidate these distinct spectral features.

For comparison, the spectrum of the gas hydrate from Nigerian margin (Neris II) is displayed in Fig. 4. Two

bands are observed at ~2570 cm^{-1} and ~2593.5 cm^{-1}. The band at ~2593.5 cm^{-1} match reasonably well with the band assigned to the H–S stretching of H_2S in the LC of the synthetic H_2S-hydrate. The absence of the band at ~2605 cm^{-1} in the natural sample may come from the low concentration of enclosed H_2S and a low signal/noise ratio. One deduces that H_2S-hydrate is present at low concentration in this specimen and H_2S is co-clathrated with methane in a type I structure.

The 2570 cm^{-1} band common to all natural hydrates may in turn originate from methane. As discussed above, no peak originating from sulfur compounds matches exactly this band. Although the contribution of HS^- ions dissolved in the water structure cannot be completely ruled out due to unknown pressure effects, evidence exists that a non-fundamental molecular vibration of methane may correspond to this peak. In Fig. 4, the spectrum of our pure synthetic CH_4-hydrate presents also a weak signal at 2570 cm^{-1}. In the free gas phase, CH_4 has no fundamental vibration in this region, but a weak band is though observed at 2580 cm^{-1}. It is tempting to attribute this vibration to the first overtone of v_4 (1306 cm^{-1}) bending mode of CH_4. Note that v_4 is very weak and is not observed by us in the methane gas phase. According to group theory, v_4 is triply degenerate and corresponds to the symmetry species F_2 (Colthup et al., 1990). We derived the spectroscopic activity of the triply degenerate overtone using the relation:

$$\chi^2_{F2}(R) = \frac{1}{3}(2\chi_{F2}(R)\chi_{F2}(R) + \chi_{F2}(R^2)),$$

where $\chi^e_{F2}(R)$ is the character of the overtone $2v_4$. Using this expression, the symmetry species of the excited state is determined as: $(F_2)^2 = A_1 + E + F_2$. All these modes being Raman active in T_d, the overtone $2v_4$ will also be active in Raman. Thus, evidence exists that the band at 2580 cm^{-1} may correspond to $2v_4$ and that this band is apparently downshifted to 2570 cm^{-1} in the hydrate due to the perturbation by water molecules. It should be noted that the assignment of triply degenerate overtones is uncertain because of anharmonicity that may result in a splitting of overtones in sub-bands whose separations and relative intensities are difficult to predict. Further work using methane isotopes is certainly needed and may help in a more definitive assignment. In contrast to v_1, no splitting due to trapping of CH_4 in the different cages is observed in the $2v_4$ spectral region. This may be rationalized by the low signal to noise ratio that prevents the observation of this mode. It should be noted that $2v_4$ (assuming a bending overtone assignment) is expected to be shifted positively in respect to the free gas phase according to the loose-cage–tight-cage model. As discussed above in the case of $2v_2$, the model is apparently unable to explain the trends in the bending frequencies of the guests and thus of the bending overtones of methane. Further work is in progress to relate our Raman results to crystallographic and thermodynamic measurements in order to give a better account of the formation and dissociation mechanisms of natural gas hydrates.

4. Summary

Micro-Raman spectroscopy proves to be a powerful tool to analyze detailed spectral features characterizing the enclathrated gas components in the natural gas hydrates. The gas hydrates collected in the different geological settings (geographically and chemically) contain a high methane concentration relative to other minor components that are found slightly dispersed in the samples. They crystallize in a type I cubic lattice structure, as also confirmed from our preliminary synchrotron diffraction results obtained on the ZaiAngo specimen. Presence of type I structure rather indicates a microbial origin for methane, at least for the specimens originating from the West African coast as also corroborated from our previous work (Charlou et al., 2004). However, detailed analysis of microscopic selected areas reveals a variation in the gas distribution among the different specimens. Additional components (like CO_2 and/or H_2S, high hydrocarbons) can be spectroscopically identified in the samples recovered from the West African coast. Evidence exists that their presence has a compositional effect on the relative cage occupancy of the methane. The H_2S and CH_4 spectral contributions in the natural hydrates have been determined by comparison with synthetic hydrates of pure H_2S, CH_4 (from both H_2O and D_2O hosts). Two bands are assigned to overtones of bending of enclathrated CH_4 and are distinct from that of enclathrated H_2S. These results may also be useful to discriminate between the contribution of occluded free methane gas and/or other higher hydrocarbons during analysis of natural hydrates on the sea floor with field Raman spectrometry.

Acknowledgments

The Centre d'Etudes et de Recherches Lasers et Applications (CERLA) is supported by the Ministère chargé de la Recherche, the Région Nord-Pas de Calais, and the Fonds Européen de Développement Economique des Régions. Gas hydrates from the Congo–Angola basin and Nigerian margin studied here were collected during the ZAIANGO (ZaiROV-Leg 2 Fuides–December 2000),

and Neris II Projects funded by TOTAL and Ifremer. Gas hydrates from the Norvegian margin were collected on Hakon Mosby Mud Volcano during the ARK XIX/3b expedition in 2003, a cooperation between Alfred Wegener Institute and Ifremer. Thanks go to H. Ondreas (ZaiAngo-Leg 2 Fluides), M. Voisset and G. Floch (NERIS II) and M. Klages and E. Sauter (ARK XIX/3b) and to the scientific parties of these three cruises who's permitted the collection of gas hydrate specimens. We are grateful to the captain, officers, crew of the different research vessels and people in charge on board of sediment coring. We are indebted to P. Dhamelincourt and J. Laureyns from LASIR (Lille), B. Champagnon from LPCML (Lyon) for their valuable discussions and time accorded on the LABRAM and XY-DILOR. We are grateful to J. M. Barnola (LGGE) for providing the high pressure cell for the gas hydrate synthesis. K. C. Hester and E. D. Sloan (CHR, Colorado School of Mines) are acknowledged for their helpful discussions. The reviewers are acknowledged for their helpful suggestions.

References

Brooks, J.M., Kennicutt, M.C., Fay, R.R., McDonald, T.J., 1988. Thermogenic gas hydrates in the gulf of Mexico. Science 225, 409.

Brunsgaard Hansen, S., Berg, R.W., Stenby, E.H., 2001. Raman spectroscopic studies of methane–ethane mixtures as a function of pressure. Appl. Spectrosc. 55, 745.

Brunsgaard Hansen, S., Berg, R.W., Stenby, E.H., 2002. How to determine the pressure of a methane-containing gas mixture by means of two weak Raman bands, ν_3 and $2\nu_2$. J. Raman Spectrosc. 33, 160.

Charlou, J.L., Donval, J.P., Fouquet, Y., Ondreas, H., Knoery, J., Cochonat, P., Levaché, D., Poirier, Y., Jean-Baptiste, P., Fourré, E., Chazallon, B., 2004. Physical and chemical characterization of gas hydrates and associated methane plumes in the Congo–Angola basin. Chem. Geol. 205, 405.

Chazallon, B., Champagnon, B., Panczer, G., Pauer, F., Klapproth, A., Kuhs, W.F., 1998. Micro-Raman analysis of synthetic air-clathrates. Eur. J. Mineral. 10, 1125.

Chazallon, B., Kuhs, W.F., 2002. In situ structural properties of N_2-, O_2- and air-clathrates by neutron diffraction. J. Chem. Phys. 117, 308.

Colthup, N.B., Daly, L.H., Wiberley, S.E., 1990. Introduction to Infrared and Raman Spectroscopy, 3rd edition. Acad. Press, New York.

Davidson, D.W., 1973. In: Franks, F. (Ed.), Water — A Comprehensive Treatise, vol. 3. Plenum Press, New York.

Davidson, D.W., Garg, S.K., Gough, S.R., Handa, Y.P., Ratcliffe, C.I., Ripmeester, J.A., Tse, J.S., 1986. Laboratory analysis of a naturally occurring gas hydrate from sediment of the Gulf of Mexico. Geochim. Cosmochim. Acta 50, 619.

Dubessy, J., Boiron, M.C., Moissette, A., Monnin, C., Sretenskaya, N., 1992. Determination of water, hydrates and pH in fluid inclusions by micro-Raman spectroscopy. Eur. J. Mineral. 4, 885.

Ferraro, J.R., Nakamoto, K., 1994. Raman Spectrometry. Academic Press, Inc., London.

Gutt, C., Asmussen, B., Press, W., Merkl, C., Casalta, H., Greinert, J., Bohrmann, G., Tse, J.S., Hüller, A., 1999. Quantum rotations in natural methane-clathrates from the Pacific sea-floor. Europhys. Lett. 48, 269.

Herzberg, G., 1991. Molecular Spectra and Molecular Structure. Infrared spectra and Raman spectra of Polyatomic molecules, vol. II. Krieger publishing company, Malabar, Florida.

Hester, K.C., White, S.N., Peltzer, E.T., Brewer, P.G., Sloan, E.D., 2006. Raman spectroscopic measurements of synthetic gas hydrates in the ocean. Mar. Chem. 98, 304.

Kisch, H.J., van den Kerkhof, A.M., 1991. CH_4-rich inclusions from quartz veins in the Valley- and-Ridge province and the anthracite fields of the Pennsylvania Appalachians. Am. Mineral. 76, 230.

Klapproth, A., 2002. Strukturuntersuchungen an Methan-und Kohlenstoffdioxid-Clathrat-Hydraten. Universität Göttingen, Doktorarbeit.

Klapproth, A., Goreshnik, E., Staykova, D., Klein, H., Kuhs, W.F., 2003. Structural studies of gas hydrates. Can. J. Phys. 81, 503.

Kuhs, W.F., Chazallon, B., Radaelli, P.G., Pauer, F., 1997. Cage occupancy and compressibility of deuterated N_2-clathrate hydrate by neutron diffraction. J. Incl. Phenom. 29, 65.

Kuhs, W.F., Chazallon, B., Klapproth, A., Pauer, F., 1998. Filling isotherms in clathrate hydrates. Rev. High Pressure Sci. Technol. 7, 1147.

Kvenvolden, K.A., 1993. Gas hydrates—geological perspective and global change. Rev. Geophys. 31, 173.

Kvenvolden, K.A., 1998. A primer on the geological occurrence of gas hydrate. In: Henriet, J.P., Mienert, J. (Eds.), Gas hydrates: relevance to world margin stability and climate change. Geological Society, London, Special Publication, vol. 137, pp. 9–30.

Kvenvolden, K.A., 1999. Potential effects of gas hydrate on human welfare. Proc. Natl. Acad. Sci., U. S. A. 96, 3420.

Kvenvolden, K.A., Lorenson, T.D., 2001. The global occurrence of natural gas hydrate. In: Paull, C.K., Dilllon, W.P. (Eds.), Natural gas hydrates. Occurrence, Distribution and Detection. Geophysical Monograph, vol. 124. AGU, Columbia, pp. 3–18.

Kvenvolden, K.A., Claypool, G.E., Threlkeld, C.N., Sloan, E.D., 1984. Geochemistry of a naturally occurring massive marine gas hydrate. Org. Geochem. 6, 703.

Lee, S.-Y., Holder, G., 2001. Methane hydrates potential as a future energy resource. Fuel Process. Technol. 71, 181–186.

McIver, R.D., 1982. Role of naturally occurring gas hydrates in sediment transport. AAPG Bull. 66, 789.

Milkov, A.V., Vogt, P.R., Crane, K., Lein, A.Y., Sassen, R., Cherkashev, G.A., 2004. Geological, geochemical, and microbial processes at the hydrate-bearing Hakon Mosby mud volcano: a review. Chem. Geol. 205 (3–4), 347.

Miller, S.L., 1969. Clathrate hydrates of air in Antarctic ice. Science 134, 489.

Nakamoto, K., 1978. Infrared and Raman Spectra of Inorganic and Coordination Compounds, 3rd ed. J. Wiley & Sons, New York.

Nisbet, E., 1990. The end of the ice age. Can. J. Earth Sci. 27, 148.

Paull, C.K., Ussler, W., Dillon, W., 1991. Is the extent of glaciation limited by marine gas-hydrates. Geophys. Res. Lett. 18, 432.

Pimentel, G.C., Charles, S.W., 1963. Infrared spectral perturbations in matrix experiments. Pure Appl. Chem. 7, 111.

Richardson, H.H., Wooldridge, P.J., Devlin, J.P., 1985. FT-IR spectra of vacuum deposited clathrate hydrates of oxiran H_2S, THF, and ethane. J. Phys. Chem. 83 (9), 4387.

Rosasco, G.J., Roedder, E., 1979. Application of a new Raman microprobe spectrometer to non-destructive analysis of sulphate and other ions in individual phases in fluid inclusions in minerals. Geochim. Cosmochim. Acta 43, 1907.

Sassen, R., McDonald, I.R., 1994. Evidence of structure H hydrate, Gulf of Mexico continental slope. Org. Geochem. 22, 1029.

Savoye, B., Cochonat, P., et al., 2000. Structure et évolution récente de l'éventail turbiditique du Zaïre: premier résultats scientifiques des missions d'explorations ZaïAngo 1 et 2 (marge Congo–Angola). C. R. Acad. Sci., Ser. 2, Sci., Terre Planètes, 331, pp. 211–220.

Schicks, J., Erzinger, J., Ziemann, M.A., 2005. Raman spectra of gas hydrates — differences and analogies to ice Ih and (gas saturated) water. Spectrochim. Acta, Part A 61, 2399.

Schrötter, H.W., Klöckner, H.W., 1979. Raman scattering cross sections in gases and liquids. In: Weber, A. (Ed.), Raman spectroscopy of gases and liquids. Springer–Verlag, Berlin, pp. 123–137.

Shoji, H., Langway, C.C., 1982. Air hydrate inclusions in fresh ice core. Nature 298, 548.

Stackelberg, M.v., 1949. Feste Gashydrate. Naturwissenshaften 36, 327.

Subramanian, S., Sloan, E.D., 2002. Trends in vibrational frequencies of guests trapped in clathrate hydrate cages. J. Phys. Chem. B 106, 4348.

Sum, A.K., Burruss, R.C., Sloan, E.D., 1997. Measurements of clathrate hydrates via Raman spectroscopy. J. Phys. Chem. B 101, 7371.

Takeya, S., Kida, M., Minami, H., Sakagami, H., Hachikubo, A., Takahashi, N., Shoji, H., Soloviev, V., Wallmann, K., Biebow, N., Obzhirov, A., Salomatin, A., Poort, J., 2006. Structure and thermal expansion of natural gas clathrate hydrates. Chem. Eng. Sci. 61, 2670.

Tulk, C.A., Ripmeester, J.A., Klug, D.D., 2000. The application of Raman spectroscopy to the study of gas hydrates. NYAS 912, 859.

Uchida, T., Hirano, T., Ebinuma, T., Narita, H., Gohara, K., Mae, S., Matsumoto, R., 1999. Raman spectroscopic determination of hydration number of methane hydrates. Env. Energy Eng. 45, 12.

Udachin, K.A., Ratcliffe, C.I., Ripmeester, J.A., 2001. Structure, composition and thermal expansion of CO_2 hydrate from single crystal X-ray diffraction measurements. J. Phys. Chem. B 105, 4200.

van der Waals, J.H., Platteuw, J.C., 1959. Clathrate solutions. Adv. Chem. Phys. 2.

Wilson, L.D., Tulk, C.A., Ripmeester, J.A., 2002. Instrumental techniques for the investigation of methane hydrates: cross-calibrating NMR and Raman spectroscopy data. Proceedings of the Fourth International Conference on Gas Hydrates, Yokohama, pp. 614–618.

Wopenka, B., Pasteris, J.D., Freeman, J.J., 1990. Analysis of individual fluid inclusions by Fourier transform infrared and Raman microspectroscopy. Geochim. Cosmochim. Acta 54, 519.

Yousuf, M., Qadri, S.B., Knies, D.L., Grabowski, K.S., Coffin, R.B., Pohlman, J.W., 2004. Novel results on structural investigations of natural minerals of clathrate hydrates. Appl. Phys. A 78, 925.